Journal of Materials Chemistry

Cite this: J. Mater. Chem., 2012, 22, 17262

www.rsc.org/materials

PAPER

# Microfabricated photocrosslinkable polyelectrolyte-complex of chitosan and methacrylated gellan gum†

Daniela F. Coutinho,‡[abcd] Shilpa Sant,‡[cde] Mojdeh Shakiba,[cdf] Ben Wang,[cd] Manuela E. Gomes,[ab] Nuno M. Neves,[ab] Rui L. Reis[ab] and Ali Khademhosseini*[cde]

*Received 5th March 2012, Accepted 19th June 2012*
**DOI: 10.1039/c2jm31374j**



Chitosan (CHT)-based polyelectrolyte complexes (PECs) have been receiving great attention for tissue engineering approaches. These hydrogels are held together by ionic forces and can be disrupted by changes in physiological conditions. In this study, we present a new class of CHT-based PEC hydrogels amenable to stabilization by chemical crosslinking. The photocrosslinkable anionic methacrylated gellan gum (MeGG) was complexed with cationic CHT and exposed to light, forming a PEC hydrogel. The chemical characterization of the photocrosslinkable PEC hydrogel by Fourier transform infrared spectroscopy (FTIR) revealed absorption peaks specific to the raw polymers. A significantly higher swelling ratio was observed for the PEC hydrogel with higher CHT content. The molecular interactions between both polysaccharides were evaluated chemically and microscopically, indicating the diffusion of CHT to the interior of the hydrogel. We hypothesized that the addition of MeGG to CHT solution first leads to a membrane formation around MeGG. Then, migration of CHT inside the MeGG hydrogel occurs to balance the electrostatic charges. The photocrosslinkable feature of MeGG further allowed the formation of cell-laden microscale hydrogel units with different shapes and sizes. Overall, this system is potentially useful for a variety of applications including the replication of microscale features of tissues for modular tissue engineering.

## Introduction

Hydrogels have been used for the development of engineered tissues, either as scaffolds for supporting cell growth[1] or as cell carrier and delivery systems,[2] mainly due to their structural similarity to the extracellular matrix (ECM) of tissues. Hydrogels resemble the ECM due to their highly hydrated three dimensional (3D) structure and diffusive transport characteristics.[3] Additionally, they can be processed under cell-compatible conditions.[4] Hydrogels typically present many functional groups (amino, carboxylic and hydroxyl groups) available for chemical modification and/or conjugation with other molecules. This allows engineering their properties such as cellular attachment, molecular response, structural integrity, biodegradability, biocompatibility, and micro/nanoscale processing.[5,6]

Various hydrogels were shown to influence cell attachment,[7] proliferation,[8] and differentiation.[9] Hence, a new class of hydrogels is currently being synthesized with the focus on replicating the microenvironmental characteristics of tissues, such as cell attachment,[4] mechanical properties,[10] and biodegradability.[11] Natural and synthetic polymers have both been previously used for the production of hydrogels.[12–14] Among these, chitosan (CHT)-based hydrogels are attractive due to the high availability of CHT from naturally renewable and inexpensive sources, its reported biocompatibility, and biodegradability by enzymes present in human tissues.[15–17] CHT is a linear polysaccharide composed of randomly distributed β-(1–4)-linked D-glucosamine and *N*-acetyl-D-glucosamine units, being positively charged at a pH of 6.3.[18] CHT can be obtained by the deacetylation of chitin and the number of amino groups is directly correlated with the degree of deacetylation.[19] CHT-based hydrogels can be formed either by chemical crosslinking through

[a]*3B's Research Group – Biomaterials, Biodegradables and Biomimetics, Dept of Polymer Engineering, University of Minho, Headquarters of the European Institute of Excellence on Tissue Engineering and Regenerative Medicine, AvePark, Taipas, 4806-909 Guimarães, Portugal*
[b]*ICVS/3B's - PT Government Associate Laboratory, Braga/Guimarães, Portugal*
[c]*Center for Biomedical Engineering, Department of Medicine, Brigham and Women's Hospital, Harvard Medical School, Cambridge, MA 02139, USA*
[d]*Harvard-MIT Division of Health Sciences and Technology, Massachusetts Institute of Technology, Cambridge, MA 02139, USA*
[e]*Wyss Institute for Biologically Inspired Engineering, Harvard University, Boston, MA 02115, USA*
[f]*Institute of Biomaterials and Biomedical Engineering, University of Toronto, ON, Canada*

† Electronic supplementary information (ESI) available: Schematics of the chemical reaction to produce fluorescein-labeled chitosan and survey spectra of the polymers obtained with X-ray photoelectron spectroscopy. See DOI: 10.1039/c2jm31374j

‡ Both authors contributed equally to this work.

the addition of organic precursors or catalysts or by physical association with small anionic molecules or large negatively charged polymer chains.[17,20] The advantages of the latter class of hydrogels are significant since they reduce the cross-reactions of the precursors in the body.[20] These hydrogels are often designated as polyelectrolyte complex (PEC) hydrogels, as polyelectrolyte chains of one polymer complex with the chains of an oppositely charged polymer.[21,22] CHT-based PEC networks have been developed with a number of anionic polymers, such as hyaluronic acid,[23] carragenan,[12,24] alginate,[25] xanthan gum,[26] and collagen.[27] Gellan gum (GG) is an anionic polysaccharide that has been applied for clinical purposes and has shown potential for tissue engineering applications, mainly due to its tunable mechanical properties and promising results in cartilage tissue engineering.[14,28–30] GG is composed of a tetrasaccharide repeating unit of two β-D-glucose, one β-D-glucuronic acid and one α-L-rhamnose.[31] PEC hydrogels of CHT and GG have been reported in the form of capsules and fibers.[32,33] However, the stability of these PEC hydrogels is dependent on physicochemical properties of the environment, such as charge density, pH and ionic strength. Thus, their behavior *in vivo* may be difficult to predict and their stability may be compromised upon implantation, as reported for other ionic hydrogels.[34]

Although hydrogels have been used to replicate the 3D structure and viscoelastic properties of tissues, recapitulating the spatial distribution of biomolecules, the mechanical properties and the tissue microarchitecture is not straightforward. Microengineered hydrogels enable replication of these *in vivo* microscale features of tissues.[35] However, most of the available microfabrication techniques require the use of a photocrosslinkable polymer. Previous reports in the literature have exploited the advantages of different polymers for modular tissue engineering by developing composite hydrogels using a photocrosslinkable polymer.[36,37] For example, poly(ethylene glycol) (PEG) was combined with methacrylated gelatin (GelMA), yielding a composite hydrogel with tunable mechanical properties.[36] Also, Xiao *et al.* developed a photocrosslinkable interpenetrating polymer network (IPN) based on GelMA and silk fibroin (SF) with tunable physical and mechanical properties.[37]

Recently, we have reported the chemical modification of GG with methacrylate groups (MeGG), yielding a hydrogel crosslinkable by both physical and chemical mechanisms.[38] Herein we present a simple way to prepare a robust photocrosslinkable PEC hydrogel using cationic CHT and anionic MeGG. It is hypothesized that carboxylate groups of MeGG would interact with the cationic amino groups of CHT, producing robust PEC hydrogels without the need for any harsh chemical precursors. To our knowledge, this is the first report on the combination of electrostatic interactions and the use of a photosensitive polymer for the fabrication of a robust PEC hydrogel. Controlling the degree of complexation and thus the interactions at a molecular level would allow for the development of customized hydrogels. The objective of this study was to fully characterize the developed hydrogels and the interactions between the two polymers in this system. We also investigated the fabrication of microscale hydrogels and assessed the biocompatibility of encapsulated rat cardiac fibroblast cells in order to explore the applicability of these hydrogels for tissue engineering.

## Results and discussion

CHT is one of the few positively charged polysaccharides from natural origin[22] and has been widely used for the development of PEC hydrogels.[12,23] Specifically, the development of GG–CHT PEC hydrogels has been reported by Yamamoto and collaborators.[33] However, the stability of these ionically crosslinked hydrogels cannot be assured *in vivo* since it is strongly dependent on the pH and ionic strength of the environment. Indeed, it has already been reported that ionic polymers, such as GG, can lose their stability as hydrogels due to the exchange of divalent ions with monovalent ions, present in higher concentrations in the physiological environment.[38] In this study, we hypothesized that the use of photocrosslinkable MeGG for the formation of CHT-based hydrogels may improve the hydrogel performance by increasing the structural stability of MeGG–CHT.

### Photocrosslinkable PEC hydrogel formation

A new class of photocrosslinkable PEC hydrogels was developed by combining two oppositely charged natural polysaccharides: cationic CHT (Fig. 1A) and anionic MeGG (Fig. 1B). CHT was dispersed in a solution of acetic acid (pH 4.06). The pH of MeGG solution, dissolved in deionized water, was 5.42. Given the $pK_a$ value of amine groups (6.4) of CHT[18] and of carboxylic acid groups (3.4–3.7) of MeGG,[39] both polymers were charged in the initial solutions. This was confirmed by the measurement of the zeta potential of the initial solutions (Fig. 1C). CHT was positively charged with a zeta potential value of about 38 mV, as a result of proton acceptance by the amino groups. MeGG was negatively charged with a zeta potential value of −17 mV. When MeGG was added to the CHT solution, the positively charged amino group interacted with the oppositely charged carboxylic group in MeGG by electrostatic interactions (Fig. 1D). Upon contact, a fast electrostatic interaction occurred (Fig. 1E), leading to an instant complexation. A solid membrane was formed at the interface of the two polymers, as previously reported.[40] The PEC hydrogel was then stabilized by UV exposure. Without the UV crosslinking it was not possible to handle the PEC hydrogels without leading to their disintegration, showing the importance of UV for their structural stability.

### Morphological, chemical and swelling properties of MeGG–CHT PEC hydrogels

Various parameters that affect PEC formation include the polymer molecular weight, polymer charge, pH of the solution, temperature and solvent used.[22,41] The effect of the ratio of the polymer on MeGG–CHT PEC formation was studied while keeping the other parameters constant. Thus, three different ratios of MeGG–CHT were studied by varying the volume of the polymer solutions: excess of MeGG (2MeGG : 1CHT), excess of CHT (1MeGG : 2CHT), and equivalent polymer ratio (1MeGG : 1CHT). It was observed for all the ratios that after PEC hydrogel formation, some amount of the CHT solution would remain uncomplexed with MeGG, while all the MeGG solution added would remain within the PEC hydrogel, as visualized in Fig. 1E. This can be explained by the zeta potential results, which showed higher charge amount on CHT than on MeGG. This suggests that the negative charges on the MeGG

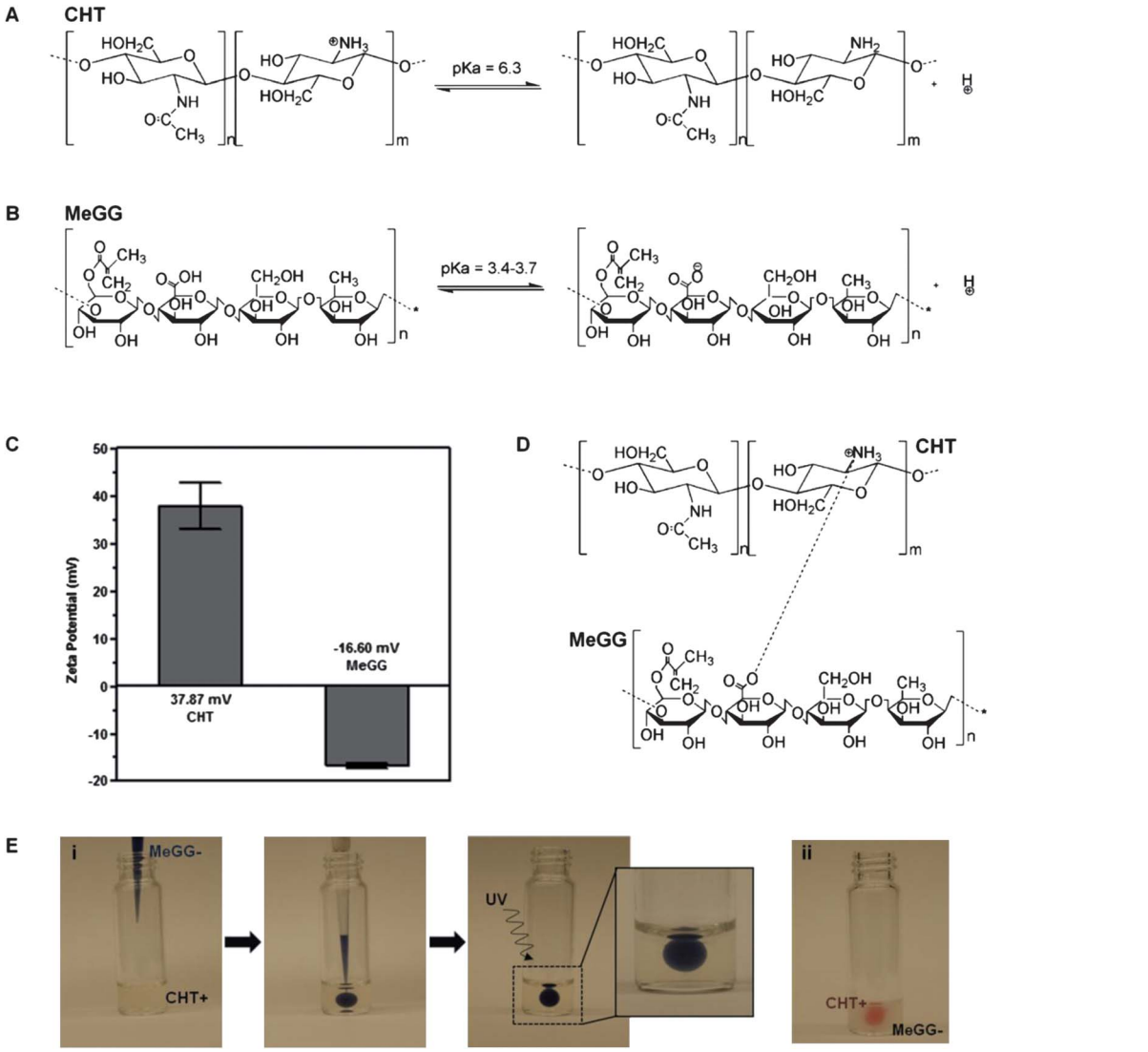


**Fig. 1** Chemical structures and illustration of the states of protonation of (A) CHT and (B) MeGG. (C) Zeta potential (mV) of CHT and MeGG in the initial solutions. (D) Representation of the possible electrostatic association between CHT and MeGG. (E) Representation of a method for the formation of photocrosslinkable PEC hydrogels by injecting (i) trypan blue stained MeGG in CHT or (ii) eosin stained CHT in MeGG solution.

readily complexed with excess positive charges on CHT chains. Although it is difficult to quantitatively measure the amount of unreacted CHT, consistent results of repeated experiments demonstrate the reproducibility of the system.

Fig. 2A shows the morphology of MeGG–CHT PEC hydrogels for MeGG : CHT ratios of 2 : 1, 1 : 1 and 1 : 2 and of the porous structure of the controls. Fibrous structures were detected along with the pores of the hydrogels for all conditions (highlighted with arrows). A similar behavior was reported by Shchipunov *et al.* when mixing CHT and xanthan gum at different ratios.[26] They observed that the morphology of the hydrogels changed from rod-like particles to a fibrillar-like structure with increasing amount of xanthan gum and thus, with higher charge ratio.[26] At the length scale analyzed, no significant change was observed in the area of the pores of the complexed hydrogels (Fig. 2B). Addition of CHT led to the formation of smaller pores as compared to pure MeGG and CHT hydrogels. This may be due to the interaction of oppositely charged polymer chains and their complexation.

FTIR-ATR of the lyophilized hydrogel was performed to characterize the chemical composition of the different polymer ratios. Fig. 3 displays the FTIR spectra of all samples. The full peak assignment is provided in Table 1. FTIR spectrum of plain CHT displayed a band at 1548 $cm^{-1}$ corresponding to the N–H bending vibration of the amine group. The absorption peak at 1409 $cm^{-1}$ was assigned to the C–N stretch of the amide. The C═O stretch of the amide group of CHT was observed at 1652 $cm^{-1}$.[42] The spectrum of the raw MeGG showed absorption peaks at 1616 $cm^{-1}$ and 1722 $cm^{-1}$ corresponding, respectively, to the C═O stretch of the carboxylic and ester groups, as previously reported.[38] When MeGG was added to the CHT solution, the absorption peaks of both CHT and MeGG were present on the spectra of the MeGG–CHT PEC hydrogels for the different ratios tested. The peaks of the carbonyl group of the carboxylic acid of MeGG in the complexed hydrogels were shifted to lower wavenumbers and presented a narrower shape. The peaks of C═O of the amide and of the ester groups were displaced to

 

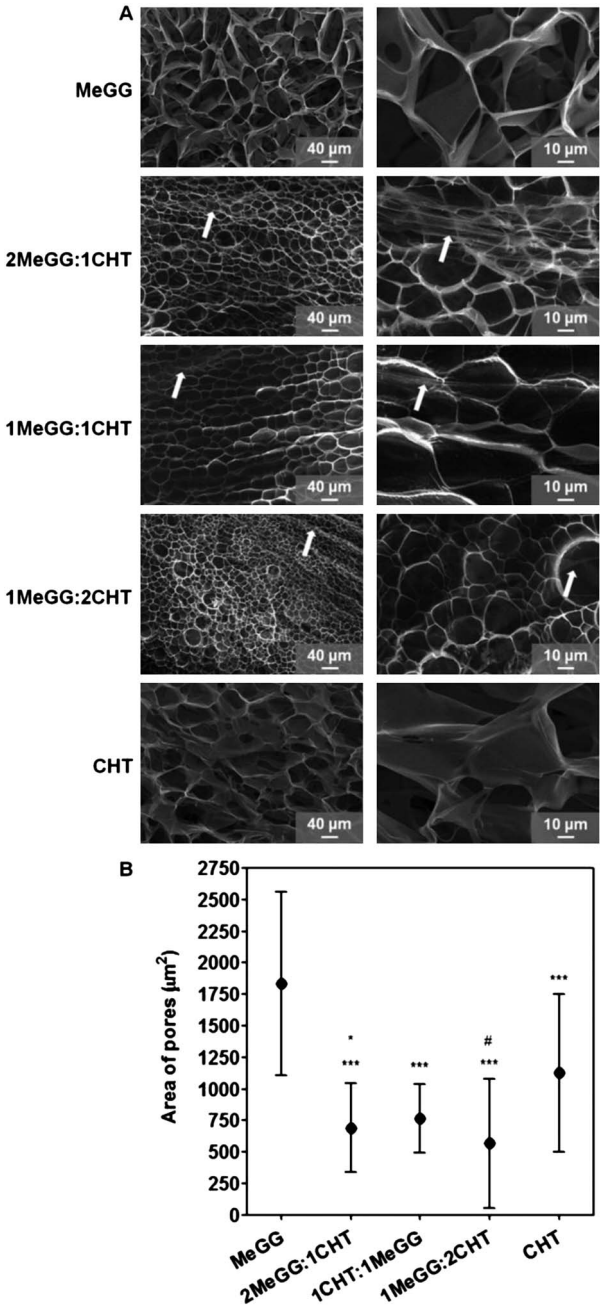


**Fig. 2** Morphological characterization of photocrosslinkable PEC hydrogels (1%, w/v) and of the controls: (A) SEM images of MeGG, 2MeGG : 1CHT, 1MeGG : 1CHT, 1MeGG : 2CHT and CHT with two magnifications (arrows indicate the presence of fibers). (B) Average area of the pores (μm²) of MeGG, MeGG–CHT and CHT hydrogels (***$p < 0.0001$, statistical difference when compared to MeGG alone; *$p < 0.05$ and #$p < 0.0001$, statistical difference when compared to CHT alone).

higher wavenumbers, indicating a chemical interaction between the two polymers. The absorption peaks of the amine on the MeGG–CHT hydrogels were shifted to lower wavenumbers from 1548 $cm^{-1}$ to 1537 $cm^{-1}$. On the complexed hydrogels a third peak appeared as a shoulder of the C=O of the carboxylic acid peak around 1589 $cm^{-1}$, possibly corresponding to the deprotonated state of the carboxylic acid ($COO^-$). The absorption bands of the C–N stretch of the amine and the C–O stretch

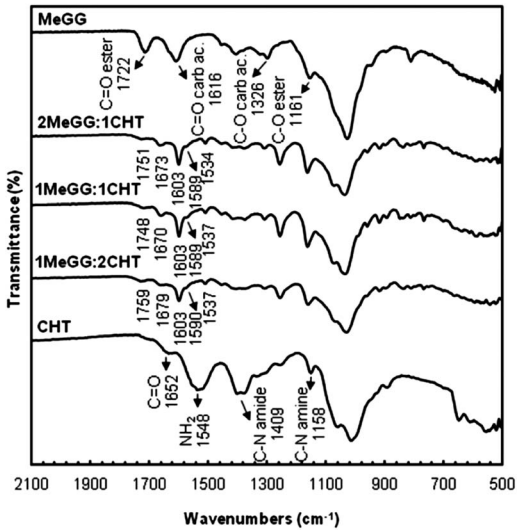


**Fig. 3** FTIR-ATR spectra of raw CHT and MeGG materials and of different volume ratios of the MeGG–CHT PEC hydrogels (2 : 1, 1 : 1 and 1 : 2).

of the ester of the complexed hydrogel overlap. FTIR spectra revealed no major differences in the position of the peaks when compared among the different ratios of MeGG and CHT.

It has been previously shown that MeGG hydrogels have tunable swelling properties,[38] presenting a rapid shrinking when immersed in ionic solutions. In the presence of ions, the formation of junction zones increases, creating more crosslinked networks and reduced degree of swelling.[43] We further investigated this behavior by immersing MeGG–CHT PEC hydrogels in PBS (containing monovalent ions) in order to assess the influence of the presence of CHT on the swelling behavior of these hydrogels (Fig. 4). After 24 h of immersion, hydrogels with the highest CHT content (1MeGG : 2CHT) presented a significantly higher (*$p < 0.05$) swelling ratio compared to MeGG alone. As previously reported,[38] the ionic crosslinking of MeGG in ionic solutions is established through the carboxylic acid group of MeGG. In the PEC hydrogel complex, the carboxylic acid group is involved in the electrostatic interactions with CHT. Thus, it is expected that with the highest CHT content, the

**Table 1** FTIR-ATR characteristic absorption bands of the components of raw CHT and MeGG and of different ratios of the MeGG–CHT PEC hydrogel (2 : 1, 1 : 1 and 1 : 2)

| Wavenumber ($cm^{-1}$) | | | | | |
|---|---|---|---|---|---|
| Functional groups | MeGG | 2MeGG : 1CHT | 1MeGG : 1CHT | 1MeGG : 2CHT | CHT |
| C–N stretch amine | — | 1168 | 1179 | 1167 | 1158 |
| C–O stretch ester | 1161 | | | | — |
| C–O stretch carboxylic acid | 1326 | 1261 | 1260 | 1263 | — |
| C–N stretch amide | — | 1423 | 1428 | 1423 | 1409 |
| $NH_2$ | — | 1534 | 1537 | 1537 | 1548 |
| C=O carboxylic acid | 1616 | 1603 | 1603 | 1603 | — |
| C=O amide | | 1673 | 1670 | 1679 | 1652 |
| C=O ester | 1722 | 1751 | 1748 | 1759 | — |

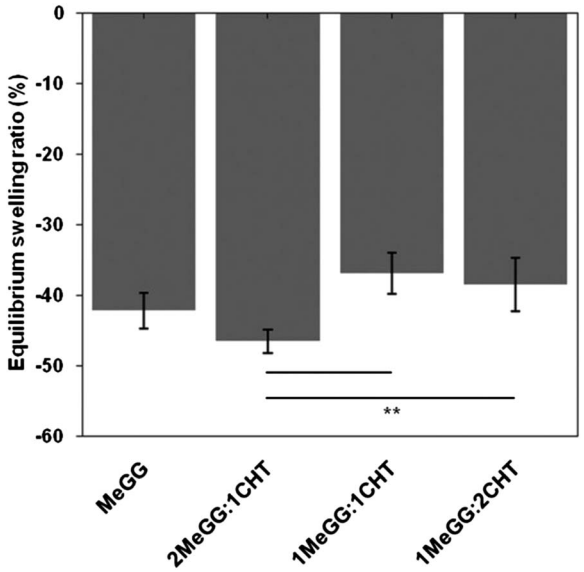


**Fig. 4** Equilibrium swelling ratio (%) of MeGG alone and MeGG–CHT hydrogels in different ratios (2 : 1, 1 : 1, 1 : 2) in PBS (**$p < 0.01$).

number of available groups for ionic crosslinking is reduced, thus decreasing the hydrogel shrinking when compared with MeGG alone. The values of the equilibrium swelling ratio of MeGG and 2MeGG : 1MeGG presented no significant differences ($p > 0.05$).

### Interactions between MeGG and CHT within the MeGG–CHT PEC hydrogel

When MeGG was added to the CHT solution, an apparent membrane started to form at the interface between both polymers. The membrane closed, forming a jellified capsule (Fig. 1E). Although CHT was involved in the formation of the membrane at the interface of the polymers, it was not clear whether CHT remained at the surface or infiltrated inside the MeGG phase. It was previously reported that when the negatively charged hyaluronic acid is added to a solution of oppositely charged peptides, a hydrogel is formed. After the hydrogel formation, the polymer chains and the peptides rearrange in order to balance the charge differences.[40] To gain more insight on the interactions between MeGG and CHT in our photocrosslinkable PEC hydrogel, the interactions at the boundary and in the bulk of the MeGG–CHT PEC hydrogel were analyzed. Only hydrogels with the same polymer ratio (1 : 1) were analyzed in this section.

PEC hydrogels were prepared for TEM immediately after fabrication. The analysis of the boundary region of the hydrogel at a nanoscale showed the presence of a membrane (Fig. 5A). To confirm the presence of CHT within the bulk hydrogel, PEC hydrogels were prepared with fluorescently labeled CHT using fluorescein. Confocal microscopy throughout the hydrogel thickness (*xz* section) one hour after hydrogel preparation confirmed the presence of CHT throughout the MeGG–CHT PEC hydrogel (Fig. 5B).

We further studied the interaction of MeGG and CHT within the PEC hydrogel by FTIR-ATR and XPS. Fig. 6A shows the FTIR-ATR spectra performed both to the surface and to the

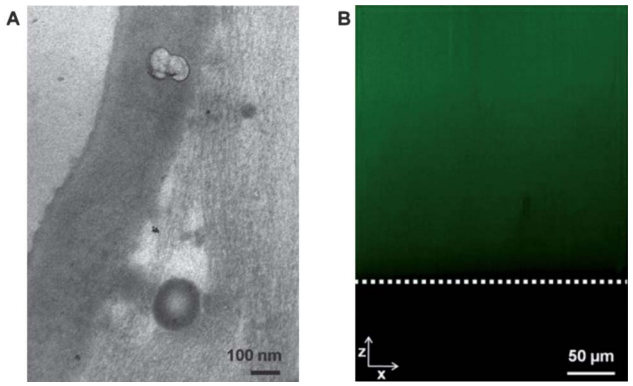


**Fig. 5** (A) TEM micrograph of photocrosslinkable MeGG–CHT PEC immersed in CHT. (B) Distribution of fluorescein-labeled CHT within the *xz* axis of the PEC MeGG–CHT capsules (white line depicts the limit of the hydrogel).

cross-section of the MeGG–CHT PEC hydrogel. The major absorption peaks of MeGG–CHT reported in Fig. 3 were also present in the cross-section of the hydrogel (Fig. 6A), indicating that the internal structure of the hydrogel had the same chemical composition as the surface. XPS chemically validated these findings. Table 2 summarizes the XPS survey scan of carbon, oxygen and nitrogen peaks of the samples. Nitrogen element was present in CHT, in agreement with the molecular structure, and also at the surface and cross-section of the MeGG–CHT PEC hydrogels. A high-resolution spectrum of nitrogen was recorded to assess the presence of different nitrogen species on the samples, namely amide, amine and protonated amine. The high-resolution N 1s spectrum of CHT could be fitted with two peaks (Fig. 6B) corresponding to the amine and amide groups of CHT, at 399.00 eV and 400.67 eV, respectively. The atomic ratios of these peaks indicated a degree of deacetylation of CHT close to 90% (Table 2). The N 1s peaks of both the surface (Fig. 6C) and section (Fig. 6D) of the MeGG–CHT PEC hydrogel were deconvoluted with a third peak corresponding to the protonated amine (401.5 eV). The presence of this peak at the surface and cross-section of the hydrogel indicated the migration of charged CHT to the interior of the hydrogel.

### Mechanism of photocrosslinkable PEC hydrogel formation

Based on the discussed results, we have formulated a possible mechanism for the PEC hydrogel formation using two large polysaccharide chains (Fig. 7). When MeGG is immersed in CHT solution, we expect the polymer chains to immediately interact upon contact. As confirmed by zeta potential measurements, both solutions were charged in the initial state. Thus, the complexation and hydrogel formation is triggered immediately once the polymer chains come in contact. As the electrostatic attraction between the positively charged CHT and negatively charged MeGG starts taking place, each protonated amine of CHT complexes with a charged carboxylic acid of the MeGG polymer, forming a physical barrier at the interface of both polymers. This physical separation between the two polymers creates a diffusion barrier for the long, coil-shaped, MeGG polymer.[31] CLSM, FTIR and XPS revealed the presence of CHT

 

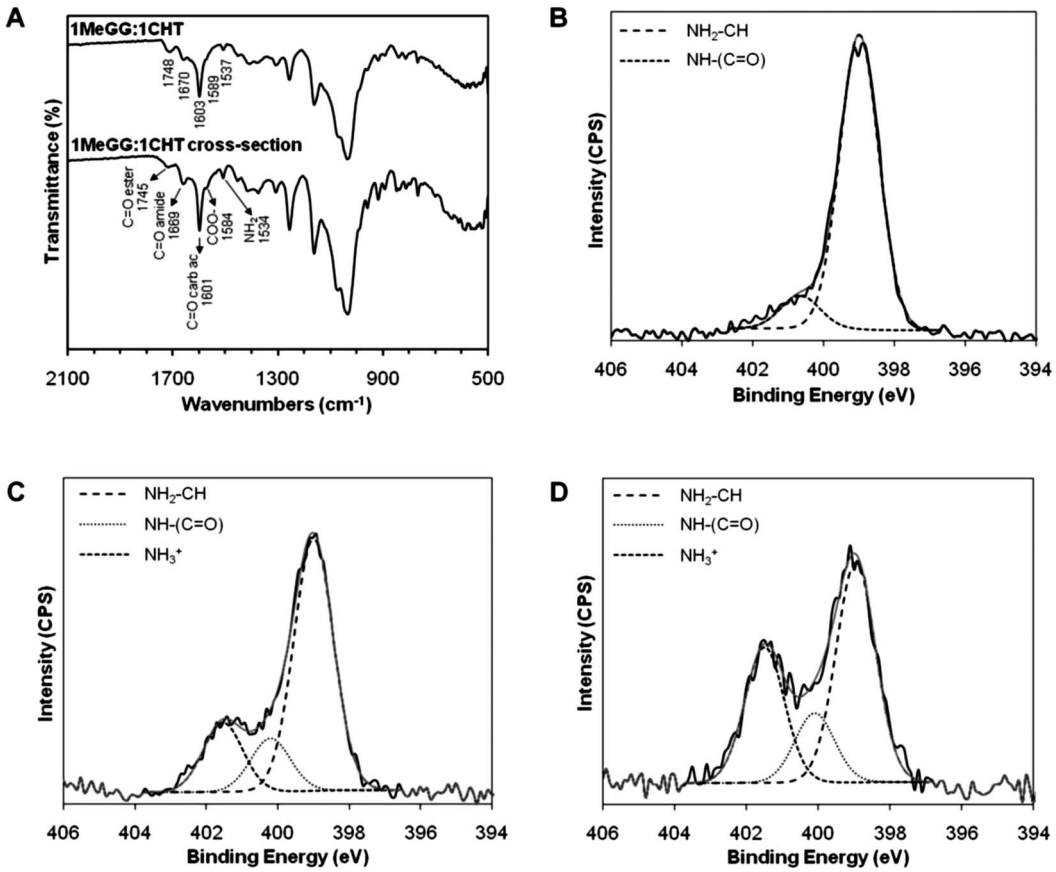


**Fig. 6** Chemical analysis of the cross-section of the MeGG–CHT PEC hydrogel with a 1 : 1 ratio. (A) FTIR-ATR spectra of the surface and cross-section of the PEC hydrogel. XPS N 1s narrow scans with the curve fit of (B) CHT, (C) surface and (D) cross-section of MeGG–CHT hydrogel. Binding energies: 399.4 ± 0.4 eV (amine), 400.5 ± 0.4 eV (amide) and 401.4 ± 0.4 eV (protonated amine).

in the interior of the hydrogel, indicating that upon the barrier formation, the polymer with a lower molecular weight would diffuse inside the hydrogel capsule. There are several parameters influencing this behavior, namely the size and configuration of the polymer chains and the charges associated with each polymer chain. The zeta potential of CHT was shown to have nearly twice as much charge as that of MeGG. We hypothesize that the highly charged CHT will migrate inside the bulk of the hydrogel in order to balance the electrostatic charges inside and outside the hydrogel. However, in each MeGG monomer, only one of the saccharides has a charged group, while CHT has, theoretically, nearly 90% of the polymeric chain charged. Thus, even though CHT migrates to the interior of the hydrogel capsule to balance the ionic charge, the atomic percent of the protonated amine inside the capsule (32%) suggests that the amount of charges of MeGG is not enough to complex with all the charged amine groups of CHT. TEM revealed the formation of a membrane-like barrier when the PEC complex was analyzed immediately after the addition of the two polymers. The hypothesized mechanism based on the results obtained from the chemical and microscopic characterizations gives an understanding over the hydrogel formation and the presence of CHT inside the bulk of the hydrogel. The structure of the MeGG–CHT PEC hydrogel can

**Table 2** Elemental analysis of the studied materials. The atomic percent of various nitrogen species was determined through curve fitting to the N 1s peak in the XPS spectra. N1 – amine (399.4 ± 0.4 eV); N2 – amide (400.5 ± 0.4 eV); N3 – protonated amine (401.4 ± 0.4 eV)

| | Elemental analysis (%) | | | Nitrogen species (%) | | |
|---|---|---|---|---|---|---|
| Materials | C 1s | O 1s | N 1s | N1 | N2 | N3 |
| CHT | 68.62 | 24.85 | 6.53 | 89.96 | 10.04 | |
| MeGG | 70.59 | 29.41 | | | | |
| MeGG–CHT section | 70.06 | 27.34 | 2.60 | 51.61 | 16.36 | 32.03 |
| MeGG–CHT surface | 70.19 | 25.48 | 4.32 | 67.25 | 14.26 | 18.50 |

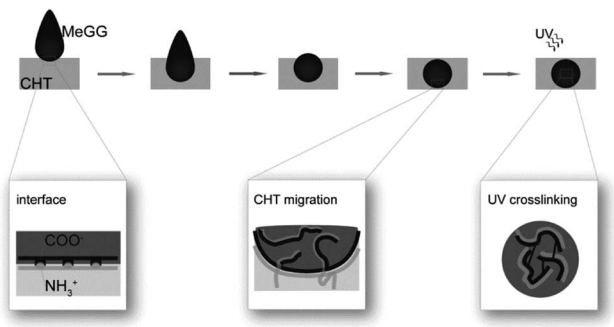


**Fig. 7** Hypothesized mechanism for the formation of a photo-crosslinkable hydrogel capsule.

be stabilized by photocrosslinking. After light exposure, the ester groups from MeGG chains covalently bond, creating a highly stable network.

### Microfabrication of fibroblast encapsulated MeGG–CHT PEC hydrogel

Microengineered blocks have been developed and assembled in order to mimic the native functional units.[44] To achieve this, different materials have been blended, forming composite hydrogel networks,[36,37] where at least one of the polymers is photocrosslinkable. We have reported a photocrosslinkable PEC that combines electrostatic interactions with photosensitive properties of polymers to develop a robust PEC hydrogel amenable to microfabrication. To demonstrate the advantage of the photocrosslinkable PEC hydrogels for tissue engineering at a microscale, MeGG–CHT hydrogels were microfabricated by photolithography into triangles and squares as an example of microfabrication into shape-specific structures. A number of microgel units could be developed merely by employing masks with different shapes (Fig. 8). The ability to wash away the uncrosslinked MeGG–CHT with pre-heated DMEM demonstrates the instability of the PEC hydrogel without the UV crosslinking. We further studied the viability of encapsulated primary fibroblasts isolated from neonatal rat hearts in micropatterned MeGG–CHT hydrogels using a Live/Dead assay. The processing method showed no significant effect over the viability of the encapsulated cells. The use of MeGG as a cell carrier protected the cells from the acidic pH of CHT, allowing encapsulation of cells inside MeGG–CHT hydrogels. It is envisioned that different types of cells can be encapsulated employing this methodology, enabling the building of heterogeneous tissues.

## Experimental

### Materials

All reagents were purchased from Sigma-Aldrich (USA), unless otherwise noted. Methacrylated gellan gum (MeGG) was synthesized as described previously.[38] Briefly, 1 g of gellan gum (GG, Gelrite®, Sigma-Aldrich, USA, $M_w$ = 1000 kDa) was dissolved in 100 mL of deionized water at 90 °C for 20–30 minutes, as described in detail elsewhere.[14] A volume of 8 mL of methacrylic anhydride (MA, Sigma) was added at 50 °C to this solution. The reaction continued for 6 hours and the pH was adjusted to 8.0 periodically with 5.0 M NaOH solution. The modified MeGG solution was purified by dialysis (Fisher Scientific, membrane with molecular weight cutoff of 11–14 kDa, USA) for at least 3 days against distilled water to remove the excess of MA. Purified MeGG was obtained by lyophilization and stored in a dry environment protected from light. Considering a degree of substitution of 11%, the average molecular weight of MeGG was calculated to be nearly 1130 kDa. Chitosan (CHT) was purchased from Sigma (degree of deacetylation of approximately 90% as determined by X-ray photoelectron spectroscopy, XPS and molecular weight of 810 kDa).

### Preparation of photocrosslinkable PEC hydrogel

CHT (1%, w/v) was dissolved in an aqueous solution of acetic acid (1%, v/v) and MeGG (1%, w/v) was dissolved in deionized

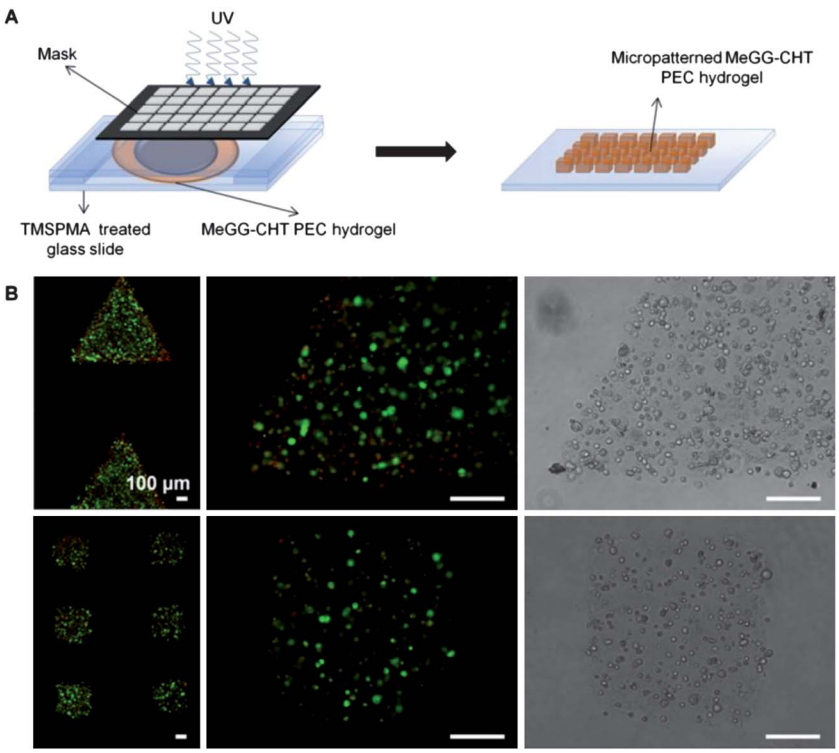


**Fig. 8** (A) Schematic of the process to create micropatterned polyelectrolyte capsules by photolithography. (B) Fluorescence images of live (green)/dead (red) fibroblasts from rat heart encapsulated in the PEC microgels microfabricated into triangles (1 h after fabrication) and squares (after 2 days in culture) (the scale bar corresponds to 100 μm).

 

water under constant stirring at 50 °C for 10 min. 0.5% (w/v) 2-hydroxy-1-[4-(2-hydroxyethoxy)phenyl]-2-methyl-1-propanone (Irgacure 2959, Ciba Specialty Chemicals) was added to the MeGG solution. The photocrosslinkable PEC hydrogel (MeGG–CHT) was formed by dispensing the negatively charged MeGG solution into the positively charged CHT solution. To visualize the formation of hydrogels, MeGG solution was colored with trypan blue and CHT solution with eosin Y. Hydrogels of CHT formed in MeGG solution were less stable since no crosslinking agent was used to stabilize the CHT hydrogel. Photocrosslinked MeGG–CHT PEC hydrogels were obtained by exposing the gel solution to light (wavelength of 320–500 nm, 7.14 mW $cm^{-2}$, EXFO OmniCure S2000) for 60 s. Hydrogels were washed with cell culture media to remove the unreacted photoinitiator. MeGG–CHT hydrogels with three different volume ratios (2 : 1, 1 : 1, 1 : 2) of the polymers were prepared by varying the volume of the two polymer solutions.

## Characterization of hydrogels

**Zeta potential measurements.** The zeta potentials of the initial solutions of MeGG and CHT (1% w/v) were determined by using a Malvern Zetasizer® 3000 HS (Malvern Instruments, UK). Each analysis was performed for 120 seconds at 25 °C. The Smoluchowski model was used with a F($K_a$) value of 1.50. Independent triplicate experiments were performed for obtaining statistical significance.

**Morphological characterization.** The morphology of the photocrosslinked MeGG–CHT PEC hydrogels (2 : 1, 1 : 1, 1 : 2 ratios and plain MeGG and CHT) was analyzed using a scanning electron microscope (SEM, Zeiss Ultra 55, Germany) with an accelerating voltage of 15 kV. Freshly prepared PEC and MeGG hydrogel samples were flash-frozen in liquid nitrogen, freeze-fractured and freeze-dried for 72 h as described previously.[45] The porous structure of CHT was obtained by flash-freezing and freeze-drying the CHT solution (1%, w/v). Freeze-dried samples were sputter coated with palladium–platinum alloy target materials with 40 mA current for 80 s using a sputter coater (SP-2 AJA Sputtering System) before SEM observation. The area of the pores of the photocrosslinked PEC hydrogels was calculated using an image analysis software (NIH Image J, $n = 40$).

**Chemical characterization.** The chemistry of the developed materials was analyzed by Fourier transform infrared spectroscopy with attenuated total reflection (FTIR-ATR). The infrared spectra were recorded using a Bruker Alpha FTIR spectrophotometer with a resolution of 4 $cm^{-1}$. The final result is presented as the average of 32 scans. X-ray photoelectron spectroscopy (XPS) enabled further chemical characterization of both the surface and the cross-section of the photocrosslinked PEC hydrogels. The analysis was performed on a Kratos Axis Ultra XPS instrument using a monochromatic Al K$\alpha$ X-ray source operating at 15 kV and 10 mA. The elements in the sample surface were identified from a survey spectrum at a pass energy of 160 eV. The areas under the specific peaks were used to calculate the atomic percentages. High-resolution spectra were also recorded at a pass energy of 20 eV and overlapping peaks were resolved into their individual components by the CasaXPS software. The component energies (399.4 ± 0.4 eV, 400.5 ± 0.4 eV and 401.4 ± 0.4 eV, respectively for amine, amide and protonated amine), number of peaks and peak widths (full width at half-maximum, fwhm, fixed for 1.2 ± 1%) were fixed initially and a refinement was performed for the peak heights only. PEC hydrogels were fabricated and freeze-dried before performing the FTIR and XPS analyses. Both the surfaces (2 : 1, 1 : 1 and 1 : 2 ratios) and the cross-section (1 : 1 ratio) of the MeGG–CHT hydrogels were evaluated. For that, a slice of the middle portion of the MeGG–CHT hydrogels was cut and freeze-dried, in order to evaluate the cross-section of the hydrogels. For the surface analysis, the MeGG–CHT hydrogels were frozen immediately after preparation.

**Swelling ratio measurement.** To assess the influence of the CHT content on the equilibrium swelling ratio of the photocrosslinked PEC hydrogels, MeGG–CHT hydrogels at 1% (w/v) with different ratios of MeGG : CHT (2 : 1, 1 : 1, 1 : 2) were immersed in 2 mL PBS at 37 °C, under mild shaking. After 24 hours, hydrogels ($n = 4$) were removed and hydrogel surfaces were quickly blotted on a filter paper. Their wet weight was measured ($w_t$) and compared to the initial wet weight ($w_0$). The equilibrium swelling ratio ($S_{eq}$) was defined in accordance with eqn (1).

$$S_{eq}(\%) = \frac{w_t - w_0}{w_0} \times 100 \quad (1)$$

## Distribution of MeGG and CHT polymers within the photocrosslinkable PEC hydrogel

The structure of the boundary region of the PEC hydrogels was observed at the nano-scale by transmission electron microscopy (TEM) immediately after preparation. PEC hydrogels were prepared (1 : 1 ratio) for analysis as described in Section 2.2. The samples were prepared by fixing hydrogels in 2% gluteraldehyde/2% paraformaldehyde and 1% osmium tetroxide. Samples were then dehydrated in acetone and embedded in epoxy resin. Ultrathin sections of 70 nm thickness were placed on TEM grids for analysis (Tecnai™ $G^2$ Spirit BioTWIN, FEI).

To evaluate the distribution of the polymers in the bulk of the PEC hydrogels, fluorescein-labeled CHT was used for the formation of the MeGG–CHT PEC hydrogels. The fluorescein–CHT conjugate was obtained as described elsewhere.[46] The chemical reaction is shown in the ESI, Fig. S1†. The pH of the CHT solution (1%, w/v) was adjusted to 6.0 with the addition of 5 M NaOH. A volume of 400 μL fluorescein solution (0.1%, w/v), previously dissolved in ethanol, was added to 10 mL of this solution. To catalyze the formation of amide bonds, 1-ethyl-3-(3-dimethylaminopropyl)carbodiimide hydrochloride (EDC, Thermo Scientific) was added to a final concentration of 0.05 M. The reaction was incubated for 12 h in the dark under stirring, at room temperature. The synthesized conjugate solution was purified by dialysis (Fisher Scientific, membrane with molecular weight cutoff of 11–14 kDa, USA) for at least 3 days against distilled water to remove the unreacted fluorescein. Purified fluorescein–CHT was obtained by lyophilization and stored in a dry environment protected from light. PEC hydrogels (1 : 1 ratio) were prepared with fluorescein–CHT between two glass slides separated by 300 μm spacers. The distribution of

fluorescein–CHT within the photocrosslinkable PEC hydrogel was evaluated by confocal laser scanning microscopy (CLSM) (Olympus FV300, Meville, NY) one hour after preparation. The imaging was initiated in the upper limit of the hydrogel and continued for a thickness of 400 μm, using 5 μm *z*-intervals. The fluorescence of fluorescein–CHT was detected upon excitation at 488 nm, through a cut-off dichroic mirror and an emission band-pass filter of 505–530 nm.

### Isolation of rat cardiac fibroblasts

Cardiac fibroblasts were isolated from the heart of a 1 day old Sprague-Dawley rat, following a procedure described in detail elsewhere.[47] Briefly, hearts ($n = 10$) were washed with Hank's balanced salt solution (HBSS, Gibco Invitrogen) and were minced and incubated in 0.3 mg $mL^{-1}$ collagenase solution containing 0.6 mg $mL^{-1}$ pancreatin (Sigma). Isolated cardiomyocytes and cardiac fibroblasts were plated in T75 flasks for 30 min in Dulbecco's Modified Eagles' medium (DMEM, Gibco Invitrogen) containing 10% of heat-inactivated fetal bovine serum (Sigma) and 1% penicillin–streptomycin (Gibco Invitrogen) at 37 °C with 5% $CO_2$. Cardiac fibroblasts were purified by removing all the non-adherent cells, including the cardiomyocytes. After reaching confluence, a cell suspension of rat cardiac fibroblasts ($10^7$ cells per mL) was prepared by trypsinization (trypsin–EDTA solution, Gibco) and incorporated into the MeGG solution previously warmed to 37 °C prior to the microfabrication.

### Microfabrication of cell-laden photocrosslinkable PEC hydrogels

The effect of PEC hydrogel formation and photocrosslinking on cell viability was assessed by encapsulating rat cardiac fibroblasts within microfabricated PEC hydrogels. MeGG–CHT hydrogels with encapsulated rat cardiac fibroblasts were micropatterned onto 3-[tris(trimethylsilyloxy)silyl]propyl methacrylate (TMSPMA) coated glass slides using photolithography methods, as previously reported.[44] Briefly, 100 μL of MeGG prepolymer containing the cell suspension (pH value of 5.4) was pipetted into the same volume of CHT previously placed on top of the TMSPMA glass slide. The untreated cover slip, placed on top of the MeGG–CHT hydrogel, was separated from the treated glass slide by 150 μm spacers. The photomask (either with triangular or square shapes) was placed directly on top of the cover slip prior to exposure to light (wavelength 320–500 nm, 7.14 mW $cm^{-2}$, EXFO OmniCure S2000). Subsequently, the cover slip was removed and the remaining uncrosslinked prepolymer cell suspension was gently washed away with preheated DMEM. Micropatterned cell-laden hydrogels were cultured for 2 days in 6-well-plates (Fisher Scientific) under standard culture conditions. The effect of the processing methodology over the viability of cells encapsulated in micropatterned MeGG–CHT hydrogels was assessed 1 h after preparation and after 2 days in culture, by incubating cells with a Live/Dead (Invitrogen) assay kit (calcein AM/ethidium homodimer-1 in DPBS) for 20 min.

### Statistical analysis

All the data were subjected to statistical analysis and were reported as mean ± standard deviation. Statistical differences ($*p < 0.05$, $**p < 0.01$, $***,^{\#}p < 0.0001$) were determined using one-way ANOVA followed by a Bonferroni post-hoc test for multiple comparisons in SEM and swelling data.

## Conclusions

Robust CHT-based PEC hydrogels were developed by combining CHT with the photocrosslinkable anionic polysaccharide MeGG. The PEC hydrogels contained fibers over the porous structure and improved the swelling behavior as compared to MeGG alone. When MeGG was added to the CHT solution, rapid electrostatic interaction occurred between the polymers at the interface, forming a membrane between both solutions. We also demonstrated the chemical interaction between CHT and MeGG in the interior of the hydrogel, indicating that CHT diffuses through the formed membrane into the bulk of the hydrogels. The ability to photocrosslink these PEC hydrogels conferred additional stability and enabled fabrication of shape-specific, cell-laden, microscale building blocks that can be used for modular tissue engineering.

## Author contribution

DFC, SS, and AK designed the study; DFC synthesized MeGG and produced the hydrogels; DFC and BW performed the SEM experiments; SS performed the FTIR experiments; DFC performed the XPS study; DFC and SS performed confocal and TEM; DFC and MS performed swelling, mechanical analysis and microfabricated hydrogels; DFC, SS and AK wrote the paper. MG, NN, and RR revised the paper; all authors discussed the results and commented on the manuscript.

## Acknowledgements

This research was funded by the US Army Engineer Research and Development Center, the Institute for Soldier Nanotechnology, the NIH (HL092836, EB007249), and the National Science Foundation CAREER award (AK). This work was partially supported by the Foundation for Science and Technology (FCT), through funds from the POCTI and/or FEDER programs and from the European Union under the project NoE EXPERTISSUES (NMP3-CT-2004-500283). DFC acknowledges the Foundation for Science and Technology (FCT), Portugal and the MIT-Portugal Program for the PhD grant SFRH/BD/37156/2007. SS acknowledges the postdoctoral fellowship awarded by Le Fonds Quebecois de la Recherche sur la Nature et les Technologies (FQRNT), Quebec, Canada and interdisciplinary training fellowship awarded by System-based Consortium for Organ Design and Engineering (SysCODE). The authors thank Dr Iva Pashkuleva and Dr Alpesh Patel for scientific discussions and Dr Maria Ericsson for technical help with TEM.

## References

1 N. C. Hunt and L. M. Grover, *Biotechnol. Lett.*, 2010, **32**(6), 733–742.
2 J. M. Rabanel, N. Bertrand, S. Sant, S. Louati and P. Hildgen, in *Polysaccharides for Drug Delivery and Pharmaceutical Applications*, ed. R. H. Marchessault, F. Ravenelle and X. Zhu, Amer Chemical Soc, Washington, 2006, p. 305.
3 M. L. Mather and P. E. Tomlins, *Regener. Med.*, 2010, **5**(5), 809–821.
4 F. Brandl, F. Sommer and A. Goepferich, *Biomaterials*, 2007, **28**(2), 134–146.

 

5 J. M. Zuidema, M. M. Pap, D. B. Jaroch, F. A. Morrison and R. J. Gilbert, *Acta Biomater.*, 2011, **7**(4), 1634–1643.
6 M. P. Lutolf and J. A. Hubbell, *Nat. Biotechnol.*, 2005, **23**(1), 47–55.
7 G. B. Schneider, A. English, M. Abraham, R. Zaharias, C. Stanford and J. Keller, *Biomaterials*, 2004, **25**(15), 3023–3028.
8 E. Hadjipanayi, V. Mudera and R. A. Brown, *J. Tissue Eng. Regener. Med.*, 2009, **3**(2), 77–84.
9 M. W. Betz, A. B. Yeatts, W. J. Richbourg, J. F. Caccamese, D. P. Coletti, E. E. Falco and J. P. Fisher, *Biomacromolecules*, 2010, **11**(5), 1160–1168.
10 A. M. Kloxin, J. A. Benton and K. S. Anseth, *Biomaterials*, 2010, **31**(1), 1–8.
11 S. B. Anderson, C. C. Lin, D. V. Kuntzler and K. S. Anseth, *Biomaterials*, 2011, **32**(14), 3564–3574.
12 A. Grenha, M. E. Gomes, M. Rodrigues, V. E. Santo, J. F. Mano, N. M. Neves and R. L. Reis, *J. Biomed. Mater. Res., Part A*, 2010, **92**(4), 1265–1272.
13 M. D. Brigham, A. Bick, E. Lo, A. Bendali, J. A. Burdick and A. Khademhosseini, *Tissue Eng. A*, 2009, **15**(7), 1645–1653.
14 J. T. Oliveira, L. Martins, R. Picciochi, P. B. Malafaya, R. A. Sousa, N. M. Neves, J. F. Mano and R. L. Reis, *J. Biomed. Mater. Res., Part A*, 2010, **93**(3), 852–863.
15 S. C. Chen, Y. C. Wu, F. L. Mi, Y. H. Lin, L. C. Yu and H. W. Sung, *J. Controlled Release*, 2004, **96**(2), 285–300.
16 N. Bhattarai, H. R. Ramay, J. Gunn, F. A. Matsen and M. Q. Zhang, *J. Controlled Release*, 2005, **103**(3), 609–624.
17 J. Berger, M. Reist, J. M. Mayer, O. Felt, N. A. Peppas and R. Gurny, *Eur. J. Pharm. Biopharm.*, 2004, **57**(1), 19–34.
18 P. Sorlier, A. Denuziere, C. Viton and A. Domard, *Biomacromolecules*, 2001, **2**(3), 765–772.
19 M. E. Gomes, H. S. Azevedo, P. B. Malafaya, S. S. Silva, J. M. Oliveira, G. A. Silva, R. A. Sousa, J. F. Mano and R. L. Reis, in *Textbook on Tissue Engineering*, ed. C. Van Blitterswijk, A. Lindahl, P. T.homsen, D. Williams, J. Hubbell and R. Cancedda, Elsevier, Amsterdam, 2007.
20 N. Bhattarai, J. Gunn and M. Q. Zhang, *Adv. Drug Delivery Rev.*, 2010, **62**(1), 83–99.
21 A. V. Ii'ina and V. P. Varlamov, *Appl. Biochem. Microbiol.*, 2005, **41**(1), 5–11.
22 S. R. Bhatia, S. F. Khattak and S. C. Roberts, *Curr. Opin. Colloid Interface Sci.*, 2005, **10**(1–2), 45–51.
23 Q. Feng, G. C. Zeng, P. H. Yang, C. X. Wang and J. Y. Cai, *Colloids Surf., A*, 2005, **257–258**, 85–88.
24 A. J. Granero, J. M. Razal, G. G. Wallace and M. I. H. Panhuis, *J. Mater. Chem.*, 2010, **20**(37), 7953–7956.
25 G. Lawrie, I. Keen, B. Drew, A. Chandler-Temple, L. Rintoul, P. Fredericks and L. Grondahl, *Biomacromolecules*, 2007, **8**(8), 2533–2541.
26 Y. Shchipunov, S. Sarin, I. Kim and C. S. Ha, *Green Chem.*, 2010, **12**(7), 1187–1195.
27 C. Deng, P. C. Zhang, B. Vulesevic, D. Kuraitis, F. F. Li, A. F. Yang, M. Griffith, M. Ruel and E. J. Suuronen, *Tissue Eng. A*, 2010, **16**(10), 3099–3109.
28 J. Carlfors, K. Edsman, R. Petersson and K. Jornving, *Eur. J. Pharm. Sci.*, 1998, **6**(2), 113–119.
29 J. T. Oliveira, T. C. Santos, L. Martins, R. Picciochi, A. P. Marques, A. G. Castro, N. M. Neves, J. F. Mano and R. L. Reis, *Tissue Eng. A*, 2009, **16**(1), 343–353.
30 A. Rozier, C. Mazuel, J. Grove and B. Plazonnet, *Int. J. Pharm.*, 1989, **57**(2), 163–168.
31 P. E. Jansson, B. Lindberg and P. A. Sandford, *Carbohydr. Res.*, 1983, **124**(1), 135–139.
32 M. Amaike, Y. Senoo and H. Yamamoto, *Macromol. Rapid Commun.*, 1998, **19**(6), 287–289.
33 K. Ohkawa, T. Kitagawa and H. Yamamoto, *Macromol. Mater. Eng.*, 2004, **289**(1), 33–40.
34 C. K. Kuo and P. X. Ma, *J. Biomed. Mater. Res., Part A*, 2008, **84**(4), 899–907.
35 A. Khademhosseini and R. Langer, *Biomaterials*, 2007, **28**(34), 5087–5092.
36 C. B. Hutson, J. W. Nichol, H. Aubin, H. Bae, S. Yamanlar, S. Al-Haque, S. T. Koshy and A. Khademhosseini, *Tissue Eng. A*, 2011, **17**(13–14), 1713–1723.
37 W. Xiao, J. He, J. W. Nichol, L. Wang, C. B. Hutson, B. Wang, Y. Du, H. Fan and A. Khademhosseini, *Acta Biomater.*, 2011, **7**, 2384–2393.
38 D. F. Coutinho, S. V. Sant, H. Shin, J. T. Oliveira, M. E. Gomes, N. M. Neves, A. Khademhosseini and R. L. Reis, *Biomaterials*, 2010, **31**(29), 7494–7502.
39 R. Mao, J. Tang and B. G. Swanson, *J. Food Sci.*, 1999, **64**(4), 648–652.
40 R. M. Capito, H. S. Azevedo, Y. S. Velichko, A. Mata and S. I. Stupp, *Science*, 2008, **319**(5871), 1812–1816.
41 S. Ulrich, M. Seijo and S. Stoll, *Curr. Opin. Colloid Interface Sci.*, 2006, **11**(5), 268–272.
42 Z. Osman and A. K. Arof, *Electrochim. Acta*, 2003, **48**(8), 993–999.
43 H. Grasdalen and O. Smidsord, *Carbohydr. Polym.*, 1987, **7**(5), 371–393.
44 Y. A. Du, E. Lo, A. Shamsher and A. Khademhosseini, *Proc. Natl. Acad. Sci. U. S. A.*, 2008, **105**(28), 9522–9527.
45 C. M. Hwang, S. Sant, M. Masaeli, N. N. Kachouie, B. Zamanian, S. H. Lee and A. Khademhosseini, *Biofabrication*, 2010, **2**(3), 035003.
46 A. M. De Campos, Y. Diebold, E. L. S. Carvalho, A. Sanchez and M. J. Alonso, *Pharm. Res.*, 2004, **21**(5), 803–810.
47 A. Khademhosseini, G. Eng, J. Yeh, P. A. Kucharczyk, R. Langer, G. Vunjak-Novakovic and M. Radisic, *Biomed. Microdevices*, 2007, **9**(2), 149–157.